RSC Advances

PAPER

View Article Online
View Journal | View Issue

Cite this: *RSC Adv.*, 2018, **8**, 25704

1,2,3-Triazole based bisphosphine, 5-(diphenylphosphanyl)-1-(2-(diphenylphosphanyl)-phenyl)-4-phenyl-1*H*-1,2,3-triazole: an ambidentate ligand with switchable coordination modes†

Latchupatula Radhakrishna, Madhusudan K. Pandey and Maravanji S. Balakrishna *

The reaction of 1-(2-bromophenyl)-4-phenyl-1*H*-1,2,3-triazole (**1**) with Ph_2PCl yielded bisphosphine, 5-(diphenylphosphanyl)-1-(2-(diphenylphosphanyl)phenyl)-4-phenyl-1*H*-1,2,3-triazole (**2**). Bisphosphine **2** exhibits ambidentate character in either the κ^2-P,N or κ^2-P,P coordination mode. Treatment of **2** with $[M(CO)_4(piperidine)_2]$ (M = Mo and W) yielded κ^2-P,N and κ^2-P,P coordinated Mo^0 and W^0 complexes $[M(CO)_4(2)]$ [M = W-κ^2-P,N (**4**); Mo-κ^2-P,P (**5**); W-κ^2-P,P (**6**)] depending on the reaction conditions. Formation and stability of κ^2-P,P coordinated Mo^0 and W^0 complexes were assessed by time dependent $^{31}P\{^1H\}$ NMR experiments and DFT studies. The complex **4** on treatment with $[AuCl(SMe_2)]$ afforded the hetero-bimetallic complex [μ-PN,P-{*o*-$Ph_2P(C_6H_4)$\{1,2,3-$N_3C(Ph)C(PPh_2AuCl)$\}-κ^2-P,N}$W(CO)_4$] (**7**). The 1 : 1 reaction between **2** and $[CpRu(PPh_3)_2Cl]$ yielded [(η^5-C_5H_5)RuCl{*o*-$Ph_2P(C_6H_4)$\{1,2,3-$N_3C(Ph)C(PPh_2)$\}}-κ^2-P,P] (**8**), whereas the similar reaction with $[Ru(\eta^6\text{-}p\text{-cymene})Cl_2]_2$ in a 2 : 1 molar ratio produced a cationic complex [(η^6-*p*-cymene)RuCl{*o*-$Ph_2P(C_6H_4)$\{1,2,3-$N_3C(Ph)C(PPh_2)$\}}-κ^2-P,N]Cl (**9**). Similarly, treatment of **2** with $[M(COD)(Cl)_2]$ (M = Pd and Pt) in a 1 : 1 molar ratio yielded Pd^{II} and Pt^{II} complexes [{*o*-$Ph_2P(C_6H_4)$\{1,2,3-$N_3C(Ph)C(PPh_2)$\}-κ^2-P,P}$PdCl_2$] (**10**) and [{*o*-$Ph_2P(C_6H_4)$\{1,2,3-$N_3C(Ph)C(PPh_2)$\}-κ^2-P,P}$PtCl_2$] (**11**). The reaction of **2** with 2 equiv. of $[AuCl(SMe_2)]$ afforded $[Au_2Cl_2$\{*o*-$Ph_2P(C_6H_4)$\{1,2,3-$N_3C(Ph)C(PPh_2)$\}\}-μ-P,P] (**12**). Most of the complexes have been structurally characterized. Palladium complex **10** shows excellent catalytic activity towards Cu-free Sonogashira alkynylation/cyclization reactions.

Received 14th May 2018
Accepted 6th July 2018

DOI: 10.1039/c8ra04086a

rsc.li/rsc-advances

Introduction

Chelating ligands having both soft- and hard-donor atoms have drawn considerable interest owing to their ability to stabilize the metal atoms before and after the oxidative addition and reductive elimination reactions, two important steps in metal mediated homogeneous catalysis.[1] If the ligands possess more than two donor atoms, and unlike pincer complexes, show flexibility in their coordination behavior to vary the donor atoms under the influence of temperature,[2] light[3] or redox reagents,[4] they can also find application in molecular switches, logic gates, sensors *etc.*[5] Therefore incorporating heteroaryl groups having donor atoms such as nitrogen, oxygen or sulphur in close proximity to phosphine moieties can generate interesting ligand systems with rich coordination chemistry.[6] In this context, mono- or bisphosphines containing pyridine,[7] imidazole,[8] pyrazole[9] or furan[10] moieties have attracted more attention, whereas triazole based systems have been less explored,[11] though they exhibit ambidentate behavior and find application in catalysis.[2,12]

Recently we reported the synthesis of two triazole based mono phosphines by exploiting the temperature controlled Li/H exchange phenomenon and studied their group 11 metals chemistry.[13] As a continuation of our work, herein, we describe the synthesis of C_1-symmetric triazole based bisphosphine **2**. We also demonstrate the ambidentate behavior of ligand **2** with Mo^0 and W^0 metal centers using extensive NMR studies and DFT calculations. The coordination chemistry of ligand **2** with Pd^{II}, Pt^{II}, Ru^{II} and Au^{I} metal precursors and the catalytic activity of palladium complex **10** in tandem Cu-free Sonagashira coupling/cyclization reactions are also investigated.

Phosphorus Laboratory, Department of Chemistry, Indian Institute of Technology Bombay, Powai, Mumbai 400076, India. E-mail: krishna@chem.iitb.ac.in; msb_krishna@iitb.ac.in; Fax: +91-22-5172-3480/2576-7152

† Electronic supplementary information (ESI) available. CCDC 1832214, 1832216–1832224. For ESI and crystallographic data in CIF or other electronic format see DOI: 10.1039/c8ra04086a

Results and discussion

Synthesis of 5-(diphenylphosphanyl)-1-(2-(diphenylphosphanyl)phenyl)-4-phenyl-1*H*-1,2,3-triazole (2)

The temperature-controlled lithiation of 1-(2-bromophenyl)-4-phenyl-1*H*-1,2,3-triazole (**1**), followed by the treatment of Ph_2PCl resulted in two different 1,2,3-triazole functionalized monophosphines [*o*-$Ph_2PC_6H_4${1,2,3-$N_3C(Ph)C(H)$}] and [C_6H_5{1,2,3-$N_3C(Ph)C(PPh_2)$}] depending on the reaction conditions.[13] This method was employed to synthesize triazole based new bisphosphine in one or two step reactions. Treatment of 1-(2-bromophenyl)-4-phenyl-1*H*-1,2,3-triazole (**1**) with two equivalents of ^{n}BuLi, followed by the addition of two equivalents of Ph_2PCl yielded bisphosphine [*o*-$Ph_2P(C_6H_4)${1,2,3-$N_3C(Ph)C(PPh_2)$}] (**2**) (Scheme 1). Alternately, 1-(2-bromophenyl)-4-phenyl-1*H*-1,2,3-triazole (**1**) on treatment with one equivalent of ^{n}BuLi followed by the addition of Ph_2PCl at −78 °C afforded kinetically stable triazole based mono phosphine **A**, which on further treatment with ^{n}BuLi followed by the addition of Ph_2PCl at room temperature produced bisphosphine [*o*-$Ph_2P(C_6H_4)${1,2,3-$N_3C(Ph)C(PPh_2)$}] (**2**) as shown in Scheme 1. The $^{31}P\{^1H\}$ NMR spectrum of **2** showed two doublets at −30.4 and −17.5 ppm with a J_{PP} coupling of 22.3 Hz. The existence of coupling between the two phosphorus atoms, which are five bonds apart, was confirmed by ^{31}P–^{31}P COSY experiment. Although, the origin of the coupling is not clear, the large $^5J_{PP}$ value indicates the least possibility of through bond coupling and does not rule out the possibility of through-space coupling. C_1-symmetric biaryl-bisphosphines[14] and imidazole based bisphosphines (Table 1) have shown through-space coupling with J_{PP} values of similar magnitude.[8b] Bischalcogenide derivatives of **2** (**2a** and **2b**; See ESI Scheme S1†) did not show phosphorus–phosphorus coupling probably due to the non-availability of phosphorus lone pairs for through space interaction, thus suggesting the coupling to be of through-space in nature. The assignment of chemical shifts in **2** are based on previously reported triazole based mono phosphines.[13] The triazole bonded phosphorus is significantly shielded compared to the *ortho*-carbon bound phosphorus atom.

Single crystals of **2** suitable for X-ray diffraction analysis were obtained from an ethanol solution of **2** kept at 0 °C for 24 h. The phosphorus centers exhibit distorted trigonal pyramidal geometry with both the phosphorus atoms being orthogonal to each other as shown in Fig. 1. The P2–C7 [1.830(3) Å] bond distance is little shorter compared to P1–C2 (1.859(3) Å) bond distances due to the better electron withdrawing nature of the triazole ring.

Coordination chemistry of bisphosphine 2

Recently, we demonstrated the coordination behavior of triazole based monophoshines towards group 11 metals, in which ligand showed mono-, di- as well as tridentate coordinating

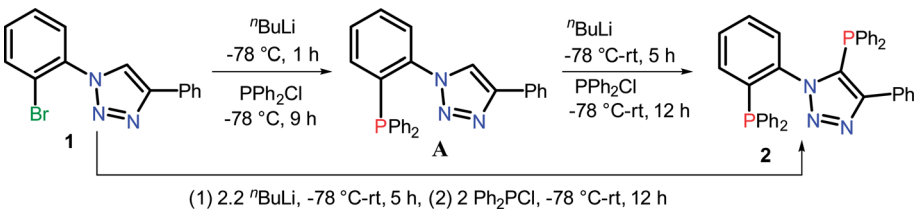

Scheme 1 Synthesis of triazole based phosphorus ligand **2**.

Table 1 The ^{31}P NMR data for C_1-symmetric bisphosphines

Compound[a]	R	δ_P[b]	J_{PP} (Hz)	Reference
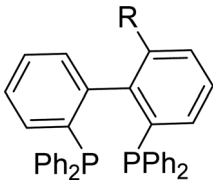	OCH_3	−13.6 (d), −14.0 (d)	18.3	14
	CH_3	−12.8 (d), −14.6 (d)	27.1	14
	Cl	−12.0 (d), −14.1 (d)	22.5	14
	C_6H_5	−13.9 (d), −15.1 (d)	11.4	14
	$N(CH_3)_2$	−14.4 (d), −14.5 (d)	5.3	14
[*o*-$Ph_2P(C_6H_4)${1-$N(CH)_2$-4-$NC(PPh_2)$}]		−18.0 (d), −30.3 (d)	24.3	8*b*
[*o*-$Ph_2P(C_6H_4)${1-$N(CH)_2$-4-$N(CH_3)C(PPh_2)$}]OTf		−19.6 (d), −22.6 (d)	27.9	8*b*
[*o*-$Ph_2P(C_6H_4)${1,2,3-$N_3C(Ph)C(PPh_2)$}] (**2**)		−17.5 (d), −30.4 (d)	22.3	This paper
[*o*-$Ph_2P(O)(C_6H_4)${1,2,3-$N_3C(Ph)C((O)PPh_2)$}] (**2a**)		28.5 (s), 12.7 (s)	[c]	This paper
[*o*-$Ph_2P(Se)(C_6H_4)${1,2,3-$N_3C(Ph)C((Se)PPh_2)$}] (**2b**)		31.6 (s) $^1J_{PSe}$ = 754 (Hz), 18.5 (s) $^1J_{PSe}$ = 752 (Hz)	[c]	This paper

[a] In all these compounds phosphorus atoms are five bonds apart. [b] δ in ppm. [c] Not observed.

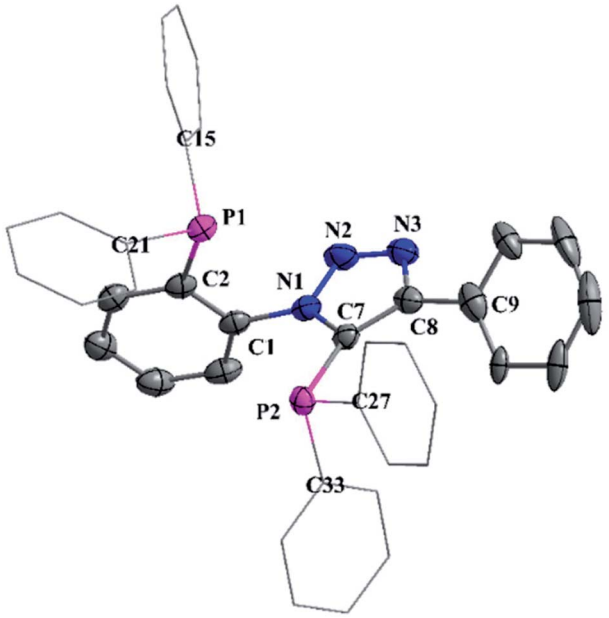

Fig. 1 Molecular structure of **2** with 50% ellipsoid probability. Hydrogen atoms were omitted for clarity. Selected bond distances (Å) and bond angles (°) of **2**: P1–C2 1.859(3), P1–C15 1.835(3), P2–C7 1.830(3), P2–C27 1.827(3), N1–N2 1.352(3), N2–N3 1.312(3), C2–P1–C15 101.42(12), C2–P1–C21 101.18(12), C15–P1–C21 103.93(12), C7–P2–C27 103.14(12), C7–P2–C33 101.64(12), C27–P2–C33 103.12(12), N1–N2–N3 106.7(2).

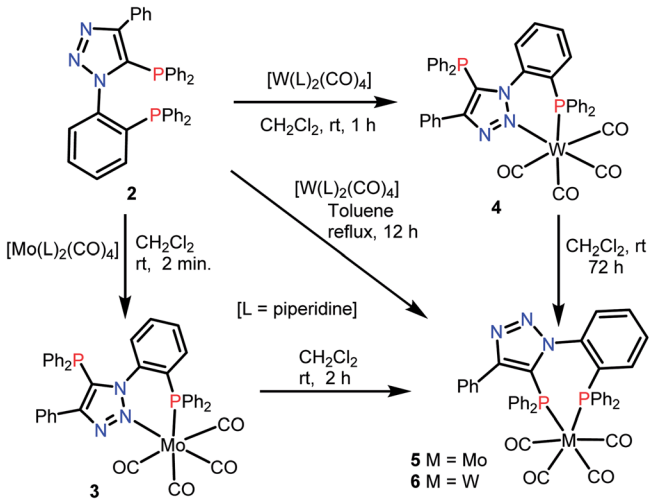

Scheme 2 Synthesis of Mo^0 and W^0 complexes **4–6**.

modes.[13] Although, bidentate mode is common with the triazole based phosphines, the reports on the participation of two nitrogen atoms in coordination is rare. Bisphosphine **2** can act as a potential tetradentate ligand. The plausible coordinating modes for the ligand **2** are listed in Chart 1. Although, simple κ^2-P,P (**I**) and κ-P, κ-P-coordination (**IV**) *via* phosphorus atoms are the most common and preferred modes for **2**, it can also show chelating [κ^2-P,N] (**II**), as well as chelating-cum-bridging [κ^2-P,N and μ-PN,P] (**III**) modes to perform as a tridentate ligand. However the possibility of **2** showing other coordinating modes **V–IX** is less likely (Chart 1), but are not precluded, as appropriate metal precursors might enable these coordination modes. Therefore, it would be interesting to study the coordination chemistry of **2** with various transition metal precursors.

Treatment of bisphosphine **2** with [Mo(piperidine)$_2$(CO)$_4$] in CH_2Cl_2 at room temperature resulted in [{*o*-$Ph_2P(C_6H_4)$}{1,2,3-$N_3C(Ph)C(PPh_2)$}-κ^2-P,P]Mo(CO)$_4$] (**5**) with ligand showing κ^2-P,P coordination. The same reaction with [W(piperidine)$_2$(CO)$_4$] afforded initially κ^2-P,N coordinated complex, [{*o*-$Ph_2P(C_6H_4)$

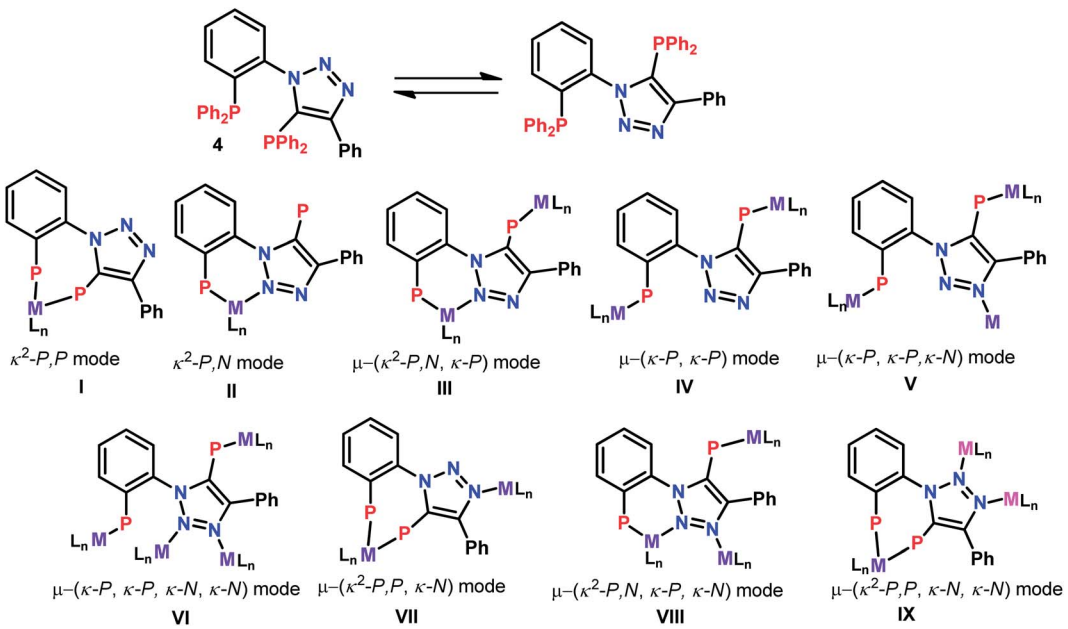

Chart 1 Possible coordinating modes for bisphosphine **2**.

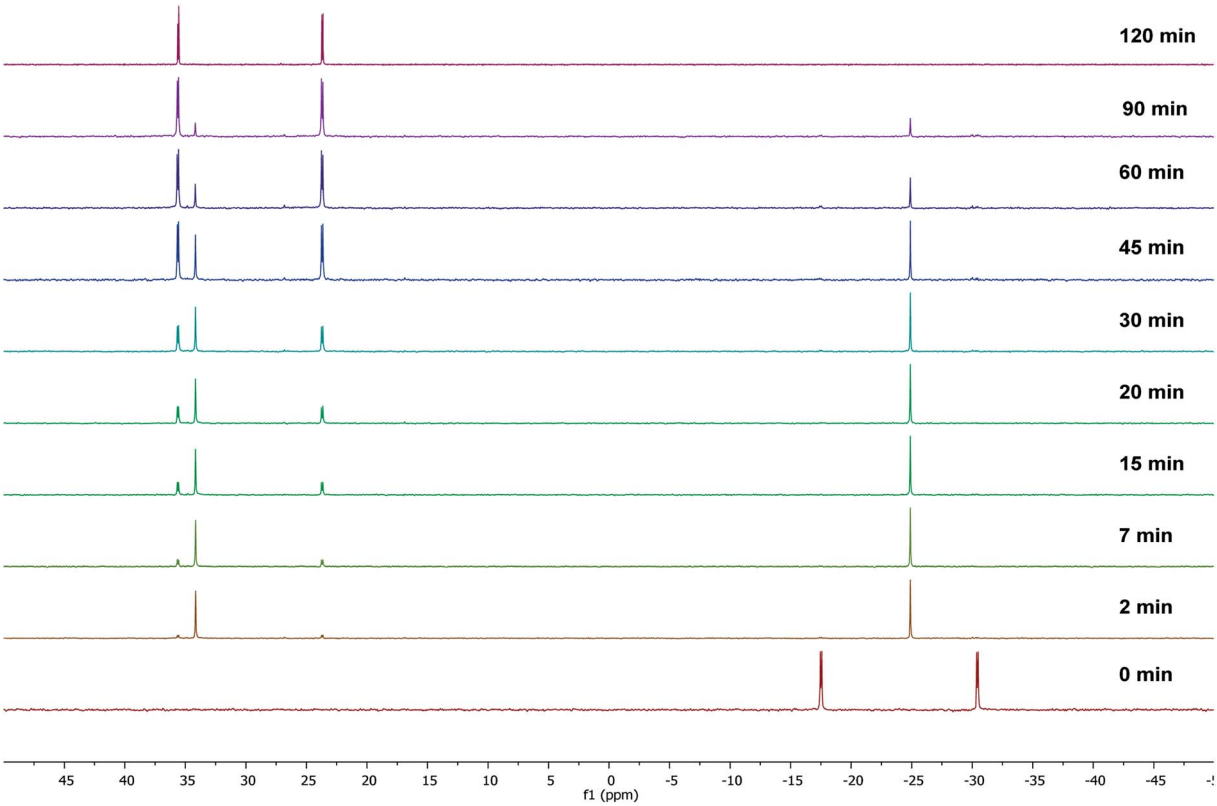

Fig. 2 Time dependent $^{31}P\{^{1}H\}$ NMR spectral data for the isomerization of complex **3** to **5**.

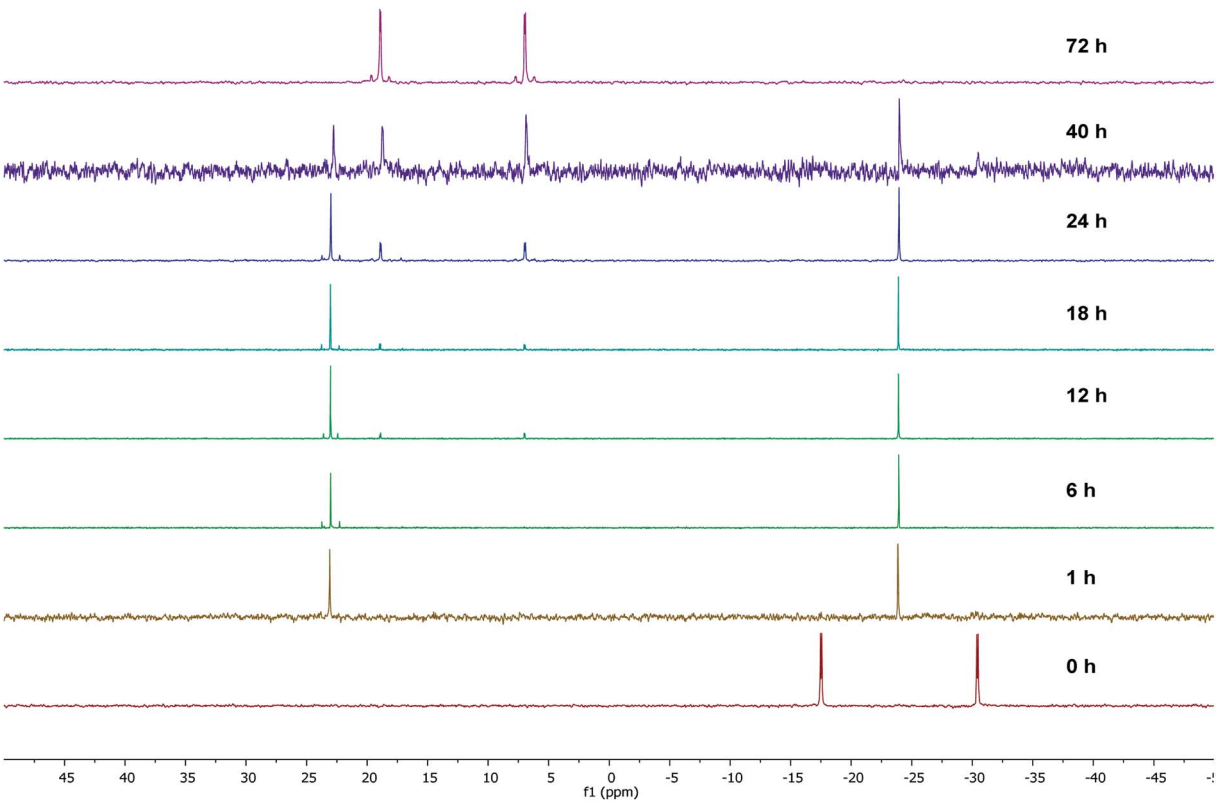

Fig. 3 Time dependent $^{31}P\{^{1}H\}$ NMR spectral data for the isomerization of complex **4** to **6**.

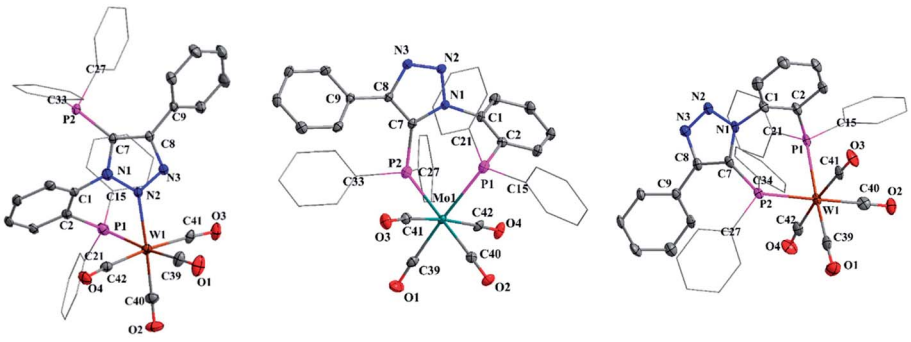

Fig. 4 Molecular structures of **4**, **5** and **6**. All hydrogen atoms and solvent molecules were omitted for clarity.

Table 2 Energy (eV) of the selected MOs and MO contributions of compounds **3–6**[a]

			Contribution of HOMO (%)			Contribution of LUMO (%)		
	HOMO (eV)	LUMO (eV)	M	CO	2	M	CO	2
3	−5.15	−1.52	60	27	13	5	4	92
4	−5.05	−1.61	56	30	14	5	4	91
5	−5.67	−1.27	64	24	12	15	4	80
6	−5.61	−1.32	60	26	14	14	5	81

[a] M = Mo (**3** and **5**), W (**4** and **6**).

{1,2,3-$N_3C(Ph)C(PPh_2)$}-κ^2-P,N}$W(CO)_4$] (**4**) which on prolonging the reaction time, yielded κ^2-P,P coordinated complex [{*o*-$Ph_2P(C_6H_4)$}{1,2,3-$N_3C(Ph)C(PPh_2)$}-κ^2-P,P}$W(CO)_4$] (**6**) as shown in Scheme 2. The complexes **4** and **5** were characterized by $^{31}P\{^1H\}$ NMR spectroscopy and their structures were confirmed by single crystal X-ray analysis. The $^{31}P\{^1H\}$ NMR spectrum of complex **4** shows two singlets at 23 ($^1J_{WP} \approx 239.2$ Hz) and −23.9 ppm, clearly indicating the coordination of aryl group bound phosphorus atom, probably along with one of the triazole nitrogen atoms and triazolyl phosphorus atom being left uncoordinated. The $^{31}P\{^1H\}$ NMR spectrum of complex **5** consists of two doublets at 35.6 and 23.7 ppm with a $^2J_{PP} \approx 19$ Hz indicating κ^2-P,P coordination to molybdenum.

To gain some insight into the stability of complexes **3** and **4**, we have examined the ΔG values obtained from DFT calculations. The energy difference (ΔG) between the κ^2-P,N coordinated W^0 complex **4** and the κ^2-P,N coordinated Mo^0 intermediate **3** is −175.1 kcal mol^{-1}, which clearly indicates relatively more stability of **4**. Similarly, the energy difference (ΔG) between the complexes **3** and **5** is −6.6 kcal mol^{-1} and the same between **4** and **6** is −6.4 kcal mol^{-1}. Therefore, the kinetically controlled κ^2-P,N-complex isomerizes to κ^2-P,P-complex. A dichloromethane solution of κ^2-P,N coordinated complex **4** on stirring at room temperature for 72 h or the reaction of **2** with $[W(piperidine)_2(CO)_4]$ in toluene under reflux conditions for 12 h yielded κ^2-P,P-complex **6** in quantitative yield. The $^{31}P\{^1H\}$ NMR spectrum of **6** shows two doublets at 18.9 ppm ($^1J_{WP} \approx 238.3$ Hz, $^2J_{PP} \approx 12.8$ Hz) and 6.9 ppm ($^1J_{WP} \approx 247.3$ Hz, $^2J_{PP} \approx 12.8$ Hz). The course of the reaction was also monitored by time dependent $^{31}P\{^1H\}$ NMR spectroscopy.

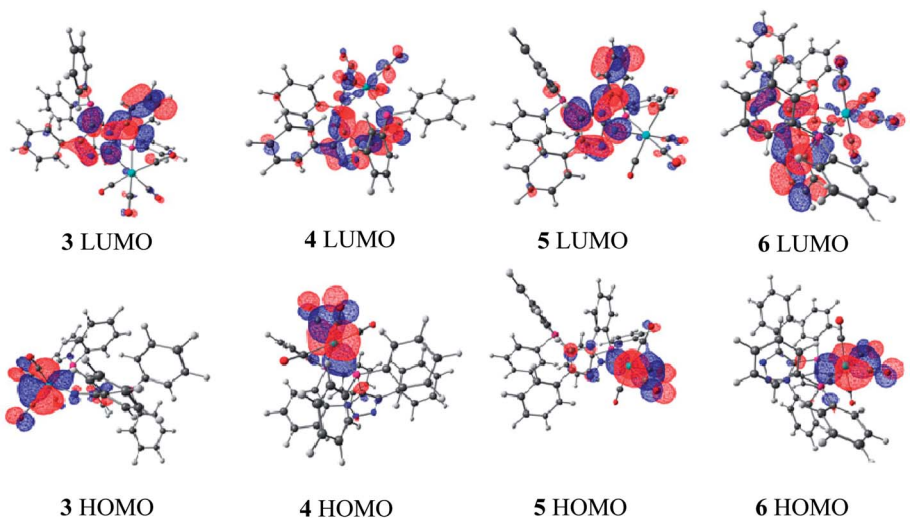

Fig. 5 Frontier molecular orbitals of compounds **3–6**.

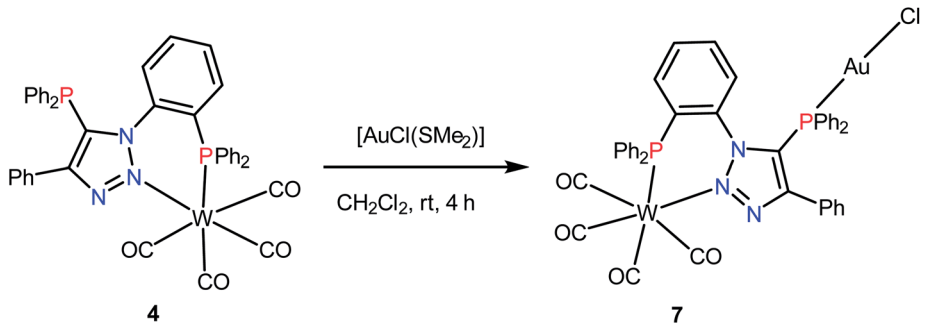

Scheme 3 Synthesis of W, Au complex 7.

Initially in the case of molybdenum, two resonances were observed at 34.1 and −24.9 ppm, corresponding to coordinated and uncoordinated phosphorus atoms indicating the formation of κ^2-P,N coordinated complex **3**. However, within 30 minutes 50% of the κ^2-P,N complex transformed into κ^2-P,P complex, and the isomerization was complete within 2 h (Fig. 2). In the case of tungsten, isomerization starts after 12 h and 50% conversion was observed after 40 h and the isomerization was complete after 72 h (Fig. 3). These NMR studies clearly show the formation of thermodynamically favored κ^2-P,P coordination complexes *via* isomerization of initially formed κ^2-P,N coordinated complexes.

The IR spectrum of complex **4** showed three ν_{CO} bands at 1850, 1887 and 2013 cm^{-1}, whereas those of **5** and **6** are appended at 1901, 2023 cm^{-1} and 1892, 2018 cm^{-1}, respectively. The ν_{CO} features are similar to those of analogous complexes of the type *cis*-$[M(CO)_4(LL)]$ (M = Mo and W; LL = dppm and dppe).[15]

The X-ray quality crystals of complexes **4–6** were obtained by solvent diffusion methods. The molecular structures of complexes **4–6** are shown in Fig. 4. The crystal structure of complex **4** reveals distorted octahedral geometry around tungsten center flanked by one of the triazolyl nitrogens (N2), phosphorus atom and four carbonyl groups. The P1–W1–N2 (75.10(9)°) angle is considerably smaller despite the formation of six-membered chelate ring which may be due to the relative orientation of N and P lone pairs. All P–Mo–C and N–Mo–C bond angles are greater than 90°, with the largest deviations being 97.74(15)° and 96.93(18)° for P1–W1–C40 and N2–W1–C39, respectively. The W–C bond distances of mutually *trans* carbonyls [W1–C41, 2.039(5) Å and W1–C42, 2.021(5) Å] are slightly longer than the W–C bond distances for the carbonyls *trans* to phosphorus and nitrogen (W1–C39 (1.972(5) Å) and W1–C40 (1.978(5) Å)), due to the poor π acceptor ability of phosphorus and triazolyl nitrogen moieties compared to the carbonyls. The P1–M–P2 bond angles in **5** and **6** are 87.76(3)° and 87.81(4)°, respectively. In **5** and **6**, the M–C bond distances for the carbonyl *trans* to the phosphorus [Mo (1.997(4) and 1.998(4) Å) and W (2.000(6) and 2.006(6))] is shorter than the M–C bond distances of mutually *trans* carbonyls [Mo (2.030(4) and 2.044(4) Å) and W (2.027(5) and 2.039(5) Å)].

In order to gain some insight into the preference between the κ^2-P,N and the κ^2-P,P coordinating modes in Mo and W–carbonyl complexes, calculations were performed using the M06/6-31G**,[16] lanl2dz level of theory[17] for complexes **3–6**. Crystal structure data were used for coordinates while performing the DFT calculations.[18] The computed geometric parameters of complexes **4–6** are in good agreement with the single crystal X-ray crystallographic structures (see ESI: Tables S1 and S2†). The HOMO and LUMO energy values are tabulated in Table 2.[19] In all these complexes, the HOMO level is majorly contributed by the metal center and carbonyl groups, whereas the LUMO level is majorly contributed by the ligand (Fig. 5).[20] The HOMO of κ^2-P,P coordinated complexes **5** and **6** are slightly higher in energy as compared to the κ^2-P,N coordinated complexes **3** and **4**.[21] The HOMO–LUMO energy differences between κ^2-P,P in **5** and **6** (4.4 eV and 4.29 eV) are even more compared to the κ^2-P,N coordinated complexes **3** and **4** (3.63 eV and 3.44 eV). It clearly suggests that the complexes **5** and **6** are more stable compared to the corresponding κ^2-P,N coordinated complexes **3** and **4**.

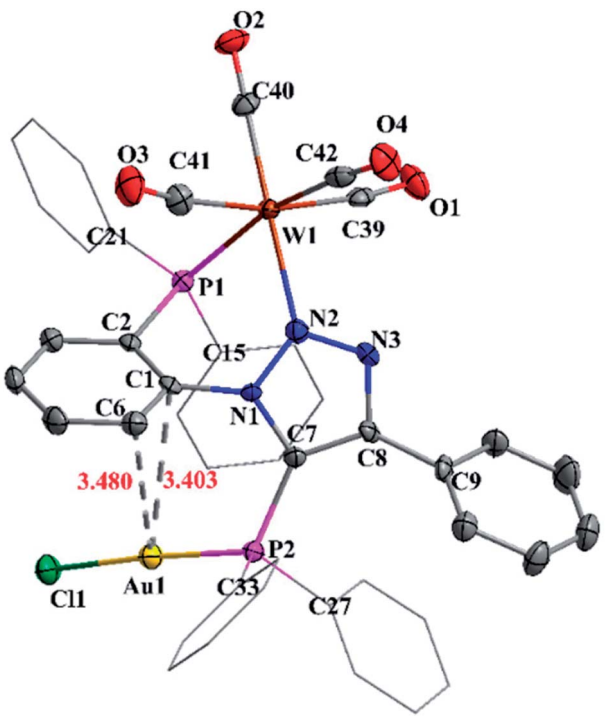

Fig. 6 Molecular structure of **7** with 50% ellipsoid probability. Hydrogen atoms were omitted for clarity.

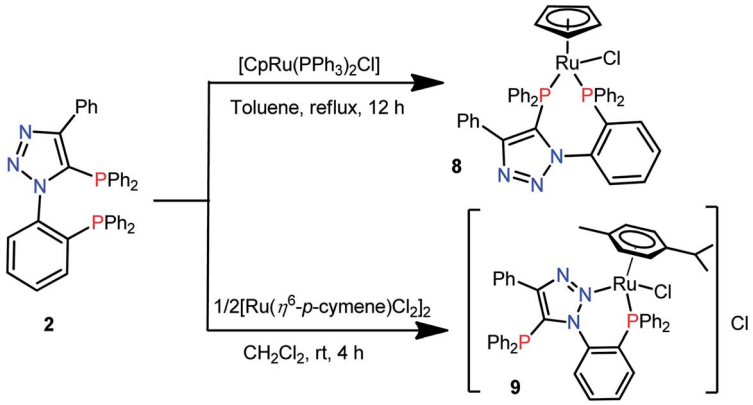

Scheme 4 Synthesis of Ru(II) complexes **8** and **9**.

The complex **4** can function as a metalloligand due to the presence of one uncoordinated phosphorus atom. The reaction of **4** with [AuCl(SMe$_2$)] in dichloromethane resulted in hetero-bimetallic complex **7** as shown in Scheme 3. The $^{31}P\{^1H\}$ NMR spectrum of **7** shows two singlets at 22.9 ($^1J_{WP} \approx 237.5$ Hz) and 12.8 ppm. A shift in the $^{31}P\{^1H\}$ NMR signal of the triazole bound phosphorus ($\Delta\delta_P = 33$) indicates its coordination to gold. The ν_{CO} of complex **7** is similar to that of **4** and shows four ν_{CO} bands at 1857, 1888 and 1901 cm^{-1} and 2010 cm^{-1}.

The molecular structure of complex **7** is shown in Fig. 6. The crystal structure of complex **7** reveals distorted octahedral geometry around tungsten and linear geometry around gold atom. The P1–W1–N2 and P1–Au1–Cl1 bond angels are 76.14(9)° and 175.86(5)°, respectively. The W1–N2 and W2–P1 bond distances are 2.244(5) Å and 2.5080(15) Å, whereas W–C bond distances vary from 1.964(6) to 2.035(6) Å. Further, complex **7** shows weak Au$\cdots$C$_{arene}$ interaction between gold and triazole (N1) attached phenyl group. The Au$\cdots$C$_{arene}$ separation is 3.40 Å for *ipso* C1 and 3.480 Å for *ortho* C6, which lies within the range of Au–C$_{arene}$ interactions (3.07–3.55 Å) reported in the literature.[22]

The reaction of bisphosphine **2** with one equvivalent of [(η^5-C$_5$H$_5$)Ru(PPh$_3$)$_2$Cl] in toluene under reflux conditions afforded mononuclear complex [(η^5-C$_5$H$_5$)RuCl{*o*-Ph$_2$P(C$_6$H$_4$)}{1,2,3-N$_3$C(Ph)C(PPh$_2$)}}-κ^2-P,P] (**8**). The $^{31}P\{^1H\}$ NMR spectrum of **8** consists of two doublets at 54.3 and 36.3 ppm with a $^2J_{PP} = 51.9$ Hz, indicating κ^2-P,P coordination. The ^{1}H NMR spectrum of **8** shows a singlet at 4.25 ppm for cyclopentadienyl protons. Reaction of **2** with 0.5 [Ru(η^6-*p*-cymene)Cl$_2$]$_2$ in dichloromethane yielded a red colored cationic complex [(η^6-*p*-cymene)RuCl{*o*-Ph$_2$P(C$_6$H$_4$)}{1,2,3-N$_3$C(Ph)C(PPh$_2$)}}-κ^2-P,N]Cl (**9**) as shown in Scheme 4. Complex **9** showed two singlets in its $^{31}P\{^1H\}$ NMR spectrum at 35.5 and −21.3 ppm, indicating κ^2-P,N coordination keeping the triazolyl phosphorus (−21.3 ppm) uncoordinated. The ^{1}H NMR spectrum of **9** showed four doublets at 6.53, 6.42, 5.92 and 5.25 ppm for the cymene group. The aliphatic protons of the cymene group showed septet at 3.10 ppm and two doublets at 1.07 and 1.24 ppm with a $^3J_{HH} = 6.5$ Hz for the isopropyl group and a singlet at 1.71 ppm for methyl group.

The crystals of complex **8** were obtained by diffusion of petroleum ether into a saturated solution of **8** in chloroform. The unit cell contains two independent molecules with identical bond parameters. In **8**, ruthenium atom adopts a pseudo-octahedral geometry (Fig. 7). The P1–Ru1–P2, P1–Ru–Cl1 and P7–Ru–Cl1 bond angels are 91.86(4), 88.72(4) and 93.59(4)°, respectively. It specifies slight deviation from the ideal octahedral angle. The Ru–P, Ru–Cl and Ru–C bond distances are in the range expected for typical half-sandwich complexes.[8c] The phosphorus (P2) attached phenyl hydrogen (H34) is involved in

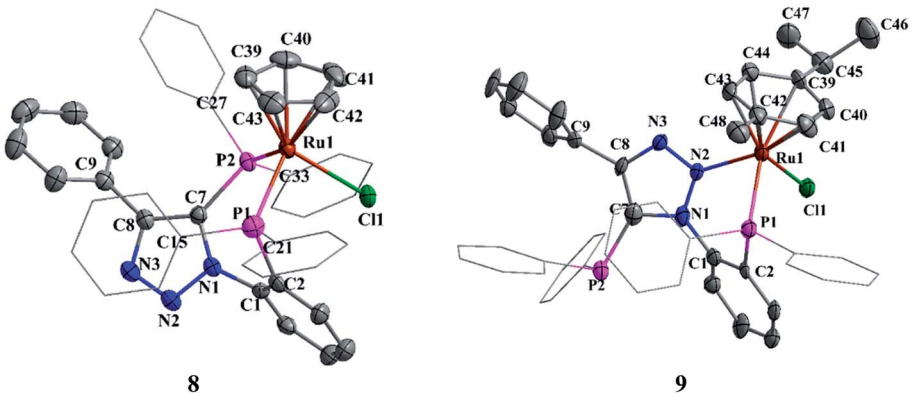

Fig. 7 Molecular structures of **8** and **9**. Hydrogen atoms and solvent molecule were omitted for clarity.

weak intermolecular hydrogen bonding with triazole nitrogen (N3) with a N3···H34 distance of 2.50 Å. This interaction plays a major role in bulk crystal packing (see ESI Fig. S1†).

In complex **9**, the ruthenium center shows pseudo-octahedral geometry with *p*-cymene, one of the nitrogen (N2) of triazole group, phosphorus atom (P2) and chloride ion occupying the coordinating sites (Fig. 7). The P1–Ru1–N2 (80.42(16)°), P1–Ru1–Cl1 (89.85(7)°) and N2–M–Cl1 (88.30(16)°) bond angles clearly indicate the distorted octahedral geometry around the ruthenium atom. The Ru1–P1, Ru1–N1 and Ru1–Cl1 bond distances are 2.3060(19), 2.136(6) and 2.4074(19) Å, respectively. The Ru1–C (2.237 Å) mean distance is comparable to the same in analogues complexes such as: [(η^6-*p*-cymene)RuCl{2-NMe$_2$-3-^{i}Pr$_2$P-indene}-κ^2-P,N]BF$_4$ (2.226 Å)[23] and [(η^6-*p*-cymene)RuCl{PR$_1$R$_2$}-κ^2-P,N]ClO$_4$ R$_1$ = (O–C$_{10}$H$_6$–C$_{10}$H$_6$–O) R$_2$ = [O–C$_6$H$_4$\{2-C(NN(Me)CH)CH\}] (2.242 Å).[24]

The reactions of [M(COD)Cl$_2$] (M = Pd, Pt) with **2** in 1 : 1 molar ratio in dichloromethane afforded [MCl$_2$(**2**)] (M = Pd (**10**); Pt (**11**)) in good yield. The ^{31}P{^{1}H} NMR spectra of **10** and **11** confirm the κ^2-P,P coordination. Interestingly palladium complex did not show $^2J_{PP}$ coupling, whereas platinum complex showed $^2J_{PP}$ and $^1J_{PtP}$ couplings of 17.52 Hz and 3582 & 3721 Hz, respectively.

The suitable crystals of complexes **10** and **11** were obtained from chloroform solution layered with petroleum ether. Both palladium and platinum atoms adopt square planar geometry (Fig. 8). The P1–M–P2 bond angles in **10** and **11** are 94.72(3)° and 94.11(16)°, respectively. Triazole nitrogen atoms N3 and N2 show weak intermolecular hydrogen bonding with phenylene hydrogen atoms H25 and H14 of two other molecules (See ESI Fig. S2†) which is evident from the N3···H25 and N2···H14 bond distances of 2.570 Å and 2.553 Å, respectively. No such interactions were observed in platinum complex **11**.

The reaction of **2** with two equivalents of [AuCl(SMe$_2$)] in dichloromethane yielded digold complex, [Au$_2$Cl$_2$\{*o*-Ph$_2$P(C$_6$H$_4$)\{1,2,3-N$_3$C(Ph)C(PPh$_2$)\}\}-μ-P,P] (**12**). The ^{31}P{^{1}H} NMR spectrum of **12** exhibits two resonances at 24.5 and 12.2 ppm. The mass spectrum of complex **12** shows a peak at 1018.0853 corresponding to [M − Cl]$^+$.

A perspective view of the molecular structure of **12** is shown in Fig. 9. The bond angels P1–Au1–Cl1 (174.94(5)°) and P2–Au2–Cl2 (174.27(4)°) are almost linear but orthogonal to each other. Au^I centers display linear geometry with an Au···Au separation of 3.3406(3) Å, indicating intramolecular aurophilic interaction. The Au···Au distance is within the range (*ca.* 2.50–3.50 Å) and less than the sum of the van der Waals radii (3.8 Å) reported in the literature.[25]

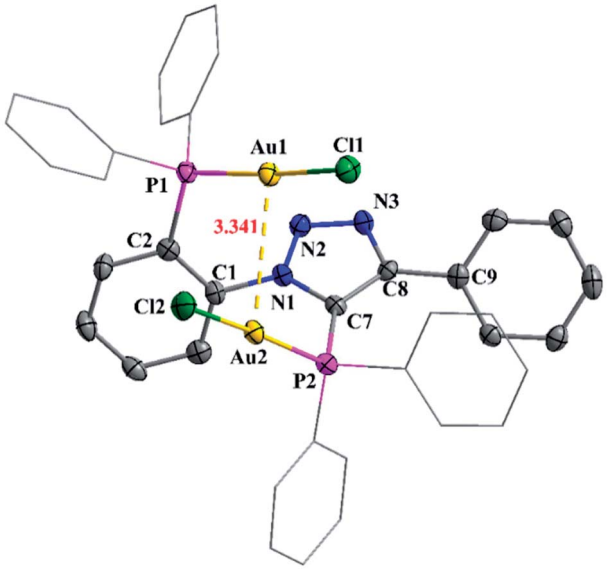

Fig. 9 Molecular structure of **12** with 50% ellipsoid probability. Hydrogen atoms and solvent molecule were omitted for clarity. Selected bond distances (Å) and bond angles (°): P1–Au1 2.2224(11), P2–Au2 2.2101(11), P1–C2 1.814(4), P2–C7 1.806(4), Au1–Cl1 2.2834(11), Au2–Cl2 2.2703(11), Au1–Au2 3.3406(3), P1–Au1–Cl1 174.27(4), P2–Au2–Cl2 174.94(5), C2–P1–Au1 115.02(15), C7–P2–Au2 111.46(14), N1–N2–N3 107.6(3).

Sonogashira coupling and sequential cyclization of alkyne and 2-halophenols to form synthetically useful 2-substituted benzofuran-type frameworks is an important methodology as these compounds constitute ubiquitous core structure in natural products and pharmaceuticals.[26] For the preparation of benzofurans, a palladium catalyst in the presence copper salt as co-catalyst is generally employed for tandem alkynylation/cyclization reactions of terminal alkynes with *o*-hydroxy aryl halides.[27] However, Cu-free Sonogashira alkynylation and sequential cyclization methods are scant in the literature.[28] In order to assess the catalytic efficiency of palladium complex **10**, tandem Cu-free Sonogashira alkynylation/cyclization reactions were performed.

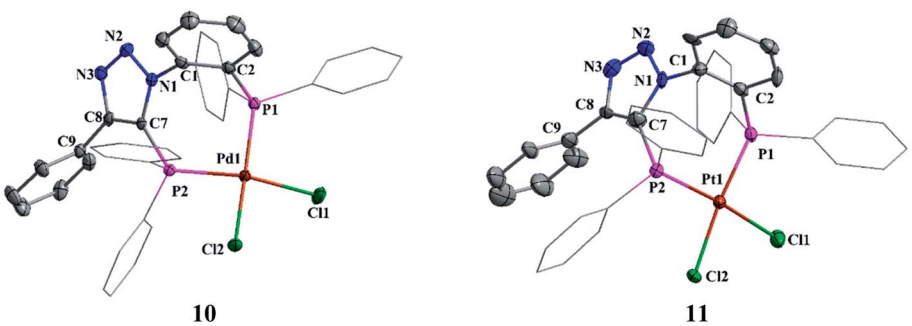

Fig. 8 Molecular structures of **10** and **11**. All hydrogen atoms and solvent molecule were omitted for clarity.

Table 3 Optimization of reaction conditions[a]

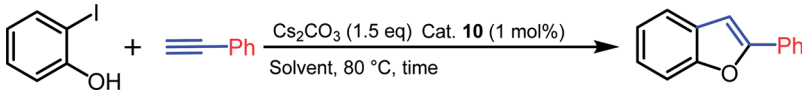

Entry	Solvent	Base	Time (h)	Conversion (%)[a]
1	Dioxane	Cs_2CO_3	12	55
2	Dioxane/H_2O(1 : 1)	Cs_2CO_3	12	68
3	CH_3CN	Cs_2CO_3	12	60
4	CH_3CN/H_2O(1 : 1)	Cs_2CO_3	12	76
5	DMF	Cs_2CO_3	12	85
6	Toluene	Cs_2CO_3	12	48
7	DMSO	K_2CO_3	12	74
8	DMSO	Cs_2CO_3	6	99 (95[b])
9	DMSO	Cs_2CO_3	12	78[c]

[a] Conversion determined by GC-MS using 2-iodophenol as internal standard. [b] Isolated yield. [c] 0.5 mol% catalyst used.

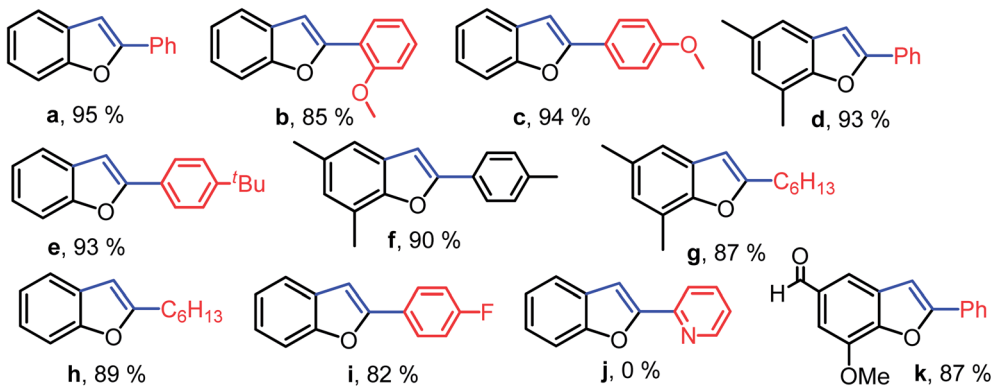

Chart 2 Substrate scope for tandem Cu-free Sonagashira alkynylation/cyclization reaction. Conditions: 2-iodophenol 0.5 mmol, alkynes 0.6 mmol, DMSO 3 mL, Cs_2CO_3 0.75 mmol, 80 °C, catalyst (1 mol%). Isolated yield.

Initially, the reaction of 2-iodophenol with phenyl acetylene was tested with 1 mol% of palladium catalyst **10** in various solvents. An excellent yield of 2-phenylbenzofuran was observed when Cs_2CO_3 was used as a base in dimethyl sulfoxide at 80 °C for 12 h. The yield was lowered considerably in other solvents (Table 3, entries 1–6). The coupling reaction was strongly influenced by the base as well as catalyst loading. Replacing Cs_2CO_3 with K_2CO_3 gave only moderate conversion (Table 3, entry 7). Catalyst loading of 0.5 mol% resulted in lower conversion rate (Table 3, entry 9). On decreasing the reaction time to 6 h, the conversion was not significantly affected (Table 3, entry 8). Under the optimized reaction conditions, various combinations of substituted *o*-iodophenols and alkynes were subjected to the tandem coupling/cyclization reaction to produce 2-substituted benzofurans in good to excellent yields. The results of the tandem Cu-free Sonogashira alkynylation/cyclization reaction are summarized in Chart 2. Both aromatic and aliphatic acetylene were tolerated in this conversion. In contrast, the coupling reaction of 2-iodophenol with 2-ethenylpyridine was not successful and resulted in negligible conversion.

Conclusions

A new triazole-based bisphosphine **2** has been synthesized. The ambidentate bisphosphine **2** shows κ^2-P,P, κ^2-P,N-chelation as well as μ-(κ^2-P,N, κ-N) and μ-(κ-P, κ-P) bridging coordination modes to act as di- or tridentate ligand. The kinetically controlled κ^2-P,N coordination modes in Mo^0 and W^0 complexes "switched" to the thermodynamically preferred κ^2-P,P coordination modes and the isomerization process was monitored by time dependent $^{31}P\{^1H\}$ NMR studies and further supported by DFT studies. The palladium complex **10** is found to be an efficient catalyst for tandem Cu-free Sonagashira alkynylation/cyclization reaction. Further catalytic investigation are under active investigation in our laboratory.

Experimental section

General procedures

All the air sensitive compounds were handled and stored in the MBRAUN Glove box. All reactions were performed under an inert atmosphere of dry nitrogen or argon, using standard

Schlenk techniques. All the solvents were dried by conventional methods and distilled prior to use. The compounds [M(piperidine)$_2$(CO)$_4$] (M = Mo and W),[33] [(η^5-C_5H_5)Ru(PPh_3)$_2$-Cl],[34] [Ru(η^6-*p*-cymene)Cl_2]$_2$,[35] [M(COD)Cl_2] (M = Pd or Pt),[36] [AuCl(SMe_2)],[37] 5-(diphenylphosphino)-1,4-diphenyl-1*H*-1,2,3-triazole,[13] 1-(2-(diphenylphosphanyl)phenyl)-4-phenyl-1*H*-1,2,3-triazole (**A**)[13] and 2-iodo-4,6-dimethylphenol[38] were prepared according to the published procedures. Other reagents were obtained from commercial sources and used after purification.

Instrumentation methods

The solution NMR spectra were recorded on a Bruker FT spectrometers (Advance-400 or 500) MHz at ambient probe temperatures. $^{13}C\{^1H\}$ and $^{31}P\{^1H\}$ NMR spectra were acquired using broad band decoupling method. The spectra were recorded in $CDCl_3$ solutions with $CDCl_3$ as an internal lock; chemical shifts of ^1H and ^{13}C NMR spectra are reported in ppm downfield from TMS, used as an internal standard. The chemical shifts of $^{31}P\{^1H\}$ NMR spectra are referred to 85% H_3PO_4 as an external standard. Positive values indicate downfield shifts. Infrared spectra were recorded on a PerkinElmer 400 FTIR instrument in KBr disk. The microanalyses were performed using a Carlo Erba Model 1112 elemental analyzer. Mass spectra were recorded using Waters Q-Tof micro (YA-105). Melting points of all compounds were determined on a Veego melting point apparatus and are uncorrected. GC-MS analyses were carried out in Agilent 7890A GC system.

Synthesis of [*o*-$Ph_2P(C_6H_4)$\{1,2,3-$N_3C(Ph)C(PPh_2)$\}] (2)

Method A. To a Schlenk flask charged with 2-bromophenyltriazole (2.5 g, 8.33 mmol) and THF (50 mL) at −78 °C, ^{n}BuLi (11.5 mL, 18.33 mmol, 1.6 M solution in hexane) was added dropwise and the reaction mixture was stirred at −78 °C for 1 hour, warmed to room temperature and stirring was continued for 4 h. The resulting reddish coloured solution was cooled to −78 °C and the THF (10 mL) solution of PPh_2Cl (3.87 g, 17.5 mmol) was added dropwise through a cannula. The resulting mixture was slowly warmed to room temperature and stirred for further 12 h and filtered through celite to remove LiCl. The solvent was removed under reduced pressure and the yellow oily residue obtained was washed with petroleum ether, dissolved in minimum amount ethanol and stored at −15 °C to get analytically pure product of **2** as a white crystalline solid. Yield: 56% (2.75 g).

Method B. To a Schlenk flask charged with 1-(2-(diphenylphosphanyl)phenyl)-4-phenyl-1*H*-1,2,3-triazole (**A**) (1 g, 2.47 mmol) in THF (40 mL) at −78 °C, was added dropwise a hexane solution of ^{n}BuLi (1.7 mL, 2.7 mmol, 1.6 M solution in hexane). The mixture was allowed to warm to room temperature and was stirred for 5 h. Again the solution was cooled to −78 °C and the THF (5 mL) solution of PPh_2Cl (0.54 g, 2.47 mmol) was added dropwise through a cannula. The resulting mixture was slowly warmed to room temperature and stirred for 12 h and LiCl was filtered off. The solvent was removed under reduced pressure and the yellow oily residue obtained was washed with petroleum ether, dissolved in minimum amount ethanol and stored at −15 °C to get analytically pure product of **2** as white crystalline solid. Yield: 62% (0.9 g).

Mp: 167–170 °C. Anal. calcd for $C_{38}H_{29}N_3P_2$: C, 77.41; H, 4.96; N, 7.13. Found C, 77.26; H, 5.38; N, 7.22% ^1H NMR (500 MHz, $CDCl_3$): δ 7.39 (td, J = 7.6, 1.3 Hz, 2H), 7.34–7.29 (m, 7H), 7.28–7.24 (m, 5H), 7.24–7.18 (m, 9H), 7.13 (dd, J = 7.3, 4.1 Hz, 4H), 7.11–7.06 (m, 1H), 7.01–6.97 (m, 2H).^{13}C NMR (126 MHz, $CDCl_3$) δ 152.69, 135.38, 133.98, 133.83, 132.92, 131.00, 130.51, 129.68, 129.27, 129.03, 128.95, 128.67, 128.61, 128.46, 127.73, 127.59. $^{31}P\{^1H\}$ NMR (202 MHz, $CDCl_3$): δ −17.52 (d, J_{PP} = 22.3 Hz), −30.43 (d, J_{PP} = 22.3 Hz). HRMS (ES) *m*/*z* calcd for $C_{38}H_{30}N_3P_2$ ([M + H]$^+$) 590.1907; found 590.1909.

Synthesis of [{*o*-$Ph_2P(C_6H_4)$\{1,2,3-$N_3C(Ph)C(PPh_2)$\}-κ^2-P,N}$W(CO)_4$] (4)

A solution of **2** (0.03 g, 0.051 mmol) and [W(CO)$_4$(piperidine)$_2$] (0.024 g, 0.051 mmol) in dichloromethane (8 mL) was stirred for 4 h at room temperature. Then, the solvent was evaporated under reduced pressure, washed with petroleum ether (3 × 5 mL) and dried under *vacuo* to give analytically pure product of **4** as a yellow solid. Yield: 80% (0.036 g). Mp: 212–215 °C. IR (KBr disk): ν_{CO} = 2013, 1887, 1850 cm^{-1}. Anal. calcd for $C_{42}H_{29}N_3O_4P_2W$: C, 56.97; H, 3.36; N, 4.75. Found C, 56.43; H, 3.68; N, 5.13%. ^1H NMR (400 MHz, $CDCl_3$): δ 7.76–7.68 (m, 2H), 7.63–7.50 (m, 10H), 7.46 (dd, J = 13.4, 5.9 Hz, 4H), 7.21 (t, J = 7.2 Hz, 1H), 7.03–6.97 (m, 1H), 6.96–6.81 (m, 7H), 6.71 (td, J = 7.8, 1.9 Hz, 2H), 6.22 (t, J = 7.5 Hz, 2H). $^{31}P\{^1H\}$ NMR (162 MHz, $CDCl_3$): δ 23.01 ($^1J_{WP}$ = 239.2), −23.94. HRMS (ES) *m*/*z* calcd for $C_{42}H_{30}N_3O_4P_2W$ ([M + H])$^+$ 886.1222; found 886.1222.

Synthesis of [{*o*-$Ph_2P(C_6H_4)$\{1,2,3-$N_3C(Ph)C(PPh_2)$\}-κ^2-P,P}$Mo(CO)_4$] (5)

A solution of **2** (0.03 g, 0.051 mmol) and [Mo(CO)$_4$(piperidine)$_2$] (0.019 g, 0.051 mmol) in dichloromethane (8 mL) was stirred for 4 h at room temperature. The solvent was evaporated under vacuum, and the residue was washed with petroleum ether (3 × 5 mL) and dried under *vacuo* to give analytically pure product of **5** as a colorless solid. Yield: 79% (0.034 g). Mp: 202–205 °C. IR (KBr disk): ν_{CO} = 2023, 1925, 1901 cm^{-1}. Anal. calcd for $C_{42}H_{29}MoN_3O_4P_2 \cdot 0.5CH_2Cl_2$: C, 60.76; H, 3.59; N, 5.00. Found C, 60.98; H, 3.67; N, 5.25%. ^1H NMR (500 MHz, $CDCl_3$): δ 7.68–7.62 (m, 2H), 7.53–7.47 (m, 2H), 7.47–7.42 (m, 3H), 7.39–7.32 (m, 5H), 7.31–7.27 (m, 4H), 7.24–7.15 (m, 5H), 7.00 (t, J = 7.4 Hz, 1H), 6.95 (dd, J = 7.7, 6.2 Hz, 1H), 6.90 (t, J = 7.7 Hz, 2H), 6.86–6.79 (m, 4H). $^{31}P\{^1H\}$ NMR (202 MHz, $CDCl_3$): δ 35.58 (d, $^2J_{PP}$ = 19.0 Hz), 23.67 (d, $^2J_{PP}$ = 19.0 Hz). HRMS (ES) *m*/*z* calcd for $C_{42}H_{30}N_3O_4P_2Mo$ ([M + H])$^+$ 800.0770; found 800.0770.

Synthesis of [{*o*-$Ph_2P(C_6H_4)$\{1,2,3-$N_3C(Ph)C(PPh_2)$\}-κ^2-P,P}$W(CO)_4$] (6)

Method A. A solution of **2** (0.03 g, 0.051 mmol) and [W(CO)$_4$(piperidine)$_2$] (0.024 g, 0.051 mmol) in dichloromethane (8 mL) was stirred for 72 h at room temperature. Then the solvent was evaporated under reduced pressure and the residue obtained was washed with petroleum ether (3 × 5 mL)

and dried under *vacuo* to give analytically pure product of **6** as colorless solid. Yield: 76% (0.034 g).

Method B. A solution of **2** (0.03 g, 0.051 mmol) and $[W(CO)_4(piperidine)_2]$ (0.024 g, 0.051 mmol) in toluene (15 mL) was refluxed for 12 h and then the reaction mixture was cooled to room temperature. The solvent was completely removed under reduced pressure and the residue obtained was washed with petroleum ether (3 × 5 mL) and dried under *vacuo* to give analytically pure product of **6** as a colorless solid Yield: 90% (0.04 g).

Mp: 217–220 °C. IR (KBr disk): ν_{CO} = 2018, 1918, 1892 cm^{-1} Anal. calcd for $C_{42}H_{29}O_4N_3P_2W$: C, 56.97; H, 3.3; N, 4.75. Found C, 56.63; H, 3.35; N, 4.57%. ^1H NMR (400 MHz, $CDCl_3$): δ 7.63 (ddd, J = 11.7, 7.5, 1.8 Hz, 2H), 7.51–7.41 (m, 5H), 7.39–7.27 (m, 8H), 7.27–7.20 (m, 5H), 7.16 (dd, J = 13.1, 5.4 Hz, 2H), 7.01 (t, J = 7.4 Hz, 1H), 6.97–6.86 (m, 3H), 6.86–6.79 (m, 3H). ^{31}P NMR (162 MHz, $CDCl_3$): δ 18.9 ($^1J_{WP}$ = 238.3 Hz, $^2J_{PP}$ = 12.8 Hz), 6.9 ($^1J_{WP}$ = 247.3 Hz, $^2J_{PP}$ = 12.8 Hz). HRMS (ES) m/z calcd for $C_{42}H_{30}N_3O_4P_2W$ ($[M + H]$)$^+$ 886.1222; found 886.1222.

Synthesis of [μ-PN,P{*o*-$Ph_2P(C_6H_4)$}{1,2,3-$N_3C(Ph)C(PPh_2AuCl)$}-κ^2-P,N}$W(CO)_4$] (7)

To a solution of complex **4** (0.051 g, 0.0576 mmol) in dichloromethane (5 mL) was added dropwise a solution of $[AuCl(SMe_2)]$ (0.017 g, 0.0576 mmol) in the same solvent (5 mL) and stirred for 4 h at room temperature. The solvent was afterward evaporated under vacuum; the residue obtained was washed with petroleum ether (2 × 5 mL) and dried under *vacuo* to give analytically pure product of **7** as an orange red solid. Yield: 84% (0.057 g). Mp: 222–225 °C. IR (KBr disk): ν_{CO} = 2010, 1901, 1888, 1857 cm^{-1} Anal. calcd for $C_{42}H_{29}AuClO_4N_3P_2W$: C, 45.12; H, 2.61; N, 3.76. Found C, 45.09; H, 2.35; N, 3.94%. ^1H NMR (500 MHz, $CDCl_3$): δ 8.10 (ddd, J = 10.8, 7.4, 2.2 Hz, 2H), 7.84–7.71 (m, 5H), 7.69–7.61 (m, 4H), 7.57 (dt, J = 6.2, 3.1 Hz, 5H), 7.23 (dd, J = 11.7, 4.4 Hz, 2H), 7.07 (ddd, J = 6.6, 5.8, 4.2 Hz, 2H), 6.92 (t, J = 7.8 Hz, 2H), 6.82 (ddd, J = 9.6, 7.3, 3.2 Hz, 3H), 6.74 (dd, J = 8.1, 1.1 Hz, 2H), 6.27 (dd, J = 14.6, 7.3 Hz, 2H). ^{31}P NMR (202 MHz, $CDCl_3$): δ 22.89 ($^1J_{WP}$ = 237.5 Hz), 12.75.

Synthesis of [(η^5-C_5H_5)RuCl{*o*-$Ph_2P(C_6H_4)$}{1,2,3-$N_3C(Ph)C(PPh_2)$}}-κ^2-P,P] (8)

A solution of $[(\eta^5\text{-}C_5H_5)Ru(PPh_3)_2Cl]$ (0.0369 g, 0.051 mmol) in toluene (8 mL) was added slowly to a solution of **2** (0.030 g, 0.051 mmol) in toluene (8 mL) at room temperature. The reaction mixture was refluxed at 100 °C for 12 h to give a clear yellow solution. The solvent was removed under vacuum and the residue obtained was washed with hot petroleum ether (3 × 8 mL) and dissolved in chloroform and layered with petroleum ether, which on slow diffusion gave red colour crystals of **8**. Yield 74% (0.03 g). Mp: 270–273 °C. Anal. calcd for $C_{43}H_{34}ClN_3P_2Ru$: C, 65.27; H, 4.33; N, 5.31. Found C, 65.41; H, 3.97; N, 5.05%. ^1H NMR (500 MHz, $CDCl_3$): δ 7.70 (s, 2H), 7.60 (dd, J = 18.2, 10.2 Hz, 3H), 7.50 (t, J = 6.5 Hz, 4H), 7.43 (s, 5H), 7.30 (t, J = 7.5 Hz, 1H), 7.26–7.20 (m, 2H), 7.19–7.10 (m, 2H), 6.93 (t, J = 7.4 Hz, 1H), 6.85 (t, J = 7.1 Hz, 1H), 6.76 (t, J = 7.1 Hz, 2H), 6.70 (t, J = 6.5 Hz, 2H), 6.66–6.60 (m, 2H), 6.45 (d, J = 7.0 Hz, 2H), 4.25 (s, 5H). $^{31}P\{^1H\}$ NMR (202 MHz, $CDCl_3$): δ 54.36 (d, J = 51.9 Hz), 36.34 (d, $^2J_{PP}$ = 51.9 Hz). HRMS (ES): m/z calcd for $C_{43}H_{35}ClN_3P_2Ru$ ($[M + H]^+$): 792.1041; found: 792.1042.

Synthesis of [(η^6-*p*-cymene)RuCl{*o*-$Ph_2P(C_6H_4)$}{1,2,3-$N_3C(Ph)C(PPh_2)$}}-κ^2-P,N]Cl (9)

A solution of $[Ru(\eta^6\text{-}p\text{-cymene})Cl_2]_2$ (0.0174 g, 0.0285 mmol) in dichloromethane (3 mL) was added drop wise to a solution of **2** (0.0338 g, 0.057 mmol) also in dichloromethane (4 mL) and stirred for 4 h at room temperature. The solvent was removed under reduced pressure and the residue obtained was washed with petroleum ether (3 × 5 mL) and dried under *vacuo* to give compound **9** as a red solid. Yield 93% (0.048 g) Mp: 257–260 °C. Anal. calcd for $C_{48}H_{43}Cl_2N_3P_2Ru$: C, 64.36; H, 4.84; N, 4.69. Found C, 64.19; H, 4.53; N, 4.36%. ^1H NMR (500 MHz, $CDCl_3$): δ 8.15 (dd, J = 12.7, 7.7 Hz, 1H), 7.88–7.62 (m, 7H), 7.57 (s, 4H), 7.48–7.40 (m, 4H), 7.34 (t, J = 7.6 Hz, 1H), 7.18–7.16 (m, 2H), 6.97 (dt, J = 40.8, 7.1 Hz, 6H), 6.73 (t, J = 7.0 Hz, 2H), 6.54 (d, J = 3.7 Hz, 1H), 6.43 (d, J = 4.7 Hz, 1H), 6.03 (t, J = 8.0 Hz, 2H), 5.93 (d, J = 6.0 Hz, 1H), 5.25 (d, J = 6.0 Hz, 1H), 3.18–3.03 (m, 1H), 1.72 (s, 3H), 1.24 (d, J = 6.5 Hz, 3H), 1.08 (d, J = 6.7 Hz, 3H). $^{31}P\{^1H\}$ NMR (202 MHz, $CDCl_3$): δ 35.52 (s), −21.34 (s). HRMS (ES): m/z Calcd. for $C_{48}H_{43}ClN_3P_2Ru$ ($[M - Cl]^+$): 860.1669; found: 860.1667.

Synthesis of [{*o*-$Ph_2P(C_6H_4)$}{1,2,3-$N_3C(Ph)C(PPh_2)$}-κ^2-P,P}$PdCl_2$] (10)

To a stirred solution of $[Pd(COD)Cl_2]$ (0.015 g, 0.051 mmol) in dichloromethane (4 mL) was added drop wise a solution of **2** (0.03 g, 0.051 mmol) also in dichloromethane (4 mL) and the reaction mixture was stirred for 4 h at room temperature. The solvent was removed under reduced pressure and the residue obtained was washed with petroleum ether (2 × 5 mL) and dried under *vacuo* to give compound **10** as a yellow solid. Yield: 85% (0.0331 g). Mp: 271–274 °C. Anal. calcd for $C_{38}H_{29}Cl_2N_3P_2Pd$: C, 59.51; H, 3.81; N, 5.48. Found C, 59.57; H, 3.44; N, 5.12%. ^1H NMR (500 MHz, $CDCl_3$): δ 8.02 (s, 2H), 7.86 (dd, J = 13.0, 7.4 Hz, 2H), 7.63 (dd, J = 11.3, 8.2 Hz, 3H), 7.57–7.49 (m, 3H), 7.48–7.41 (m, 3H), 7.33 (dd, J = 12.1, 7.8 Hz, 5H), 7.23 (d, J = 7.6 Hz, 1H), 7.18–7.10 (m, 2H), 7.09–7.02 (m, 2H), 6.99 (t, J = 7.6 Hz, 2H), 6.85 (td, J = 7.8, 3.2 Hz, 2H), 6.62 (d, J = 7.2 Hz, 2H). $^{31}P\{^1H\}$ NMR (202 MHz, $CDCl_3$): δ 25.9 (s), 12.9 (s). HRMS (ES) m/z calcd for $C_{38}H_{29}N_3P_2PdCl$ ($[M - Cl]$)$^+$ 730.0565; found 730.0565.

Synthesis of [{*o*-$Ph_2P(C_6H_4)$}{1,2,3-$N_3C(Ph)C(PPh_2)$}-κ^2-P,P}$PtCl_2$] (11)

A solution of $Pt(COD)Cl_2$ (0.019 g, 0.051 mmol) in dichloromethane (4 mL) was added drop wise to a solution of **2** (0.03 g, 0.051 mmol) also in dichloromethane (4 mL) and the solution was stirred for 4 h at room temperature. The solvent was removed under reduced pressure and the residue obtained was washed with petroleum ether (2 × 5 mL) and concentrated to a small bulk and 2 mL of chloroform was added and stored at 25 °C to give **11** as a colorless crystalline solid. Yield: 79% (0.0362 g). Mp: 260–263 °C. Anal. calcd for

Table 4 Crystallographic Information for compounds **2** and **4–7**

	2	**4**	**5**	**6**	**7**
Formula	$C_{38}H_{29}N_3P_2$	$C_{42}H_{29}N_3O_4P_2W$	$C_{43}H_{30}Cl_3MoN_3O_4P_2$	$C_{43}H_{30}Cl_3N_3O_4P_2W$	$C_{42}H_{29}AuClN_3O_4P_2W$
Formula weight	589.58	885.47	916.93	1004.84	1117.89
T (K)	150	150	150	100	150
Crystal system	Monoclinic	Triclinic	Monoclinic	Monoclinic	Monoclinic
Space group	$P2_1/n$	$P\bar{1}$	$P2_1/c$	$P2_1/c$	$P2_1/n$
a, Å	15.5170(11)	12.6150(6)	14.1841(3)	14.1865(3)	12.5915(3)
b, Å	11.9307(7)	13.3420(9)	11.2966(2)	11.2881(3)	20.0214(6)
c, Å	18.3226(15)	14.0151(8)	25.2699(6)	25.1974(9)	15.3286(4)
α, deg	90	71.437(5)	90	90	90
β, deg	111.801(9)	69.756(5)	97.008(2)	97.169(2)	92.147(2)
γ, deg	90	65.940(5)	90	90	90
V, Å^3	3149.4(4)	1977.1(2)	4018.80(15)	4003.53(19)	3861.62(18)
Z	4	2	4	4	4
ρ_{calc}g/cm^3	1.243	1.487	1.515	1.667	1.923
M (MoKα)/mm^{-1}	0.169	3.046	0.653	3.213	6.97
F(000)	1232	876	1856	1984	2136
Crystal size (mm^3)	0.151 × 0.14 × 0.065	0.171 × 0.146 × 0.108	0.314 × 0.154 × 0.095	0.224 × 0.119 × 0.097	0.168 × 0.053 × 0.039
Theta range (deg)	4.33 to 49.994	4.082 to 50	4.624 to 49.998	3.958 to 49.996	4.112 to 49.998
Reflections collected	21 113	22 276	42 569	21 398	18 829
Independent reflections	5544	6935	7077	6857	6764
S	1.059	1.054	1.033	1.04	1.034
R_1[a]	0.0555	0.0336	0.0472	0.0379	0.0323
wR_2[b]	0.1586	0.0861	0.1198	0.0949	0.0781

[a] $R = \Sigma||F_o| - |F_c||/\Sigma|F_o|$. [b] $wR_2 = [\Sigma w(F_o^2 - F_c^2)^2/\Sigma w(F_o^2)^2]^{1/2}$ w $= 1/[\sigma^2(F_o^2) + (xP)^2]$ where $P = (F_o^2 + 2F_c^2)/3$.

$C_{38}H_{29}Cl_2N_3P_2Pt\cdot 0.5CH_2Cl_2$: C, 51.49; H, 3.37; N, 4.68. Found C, 51.70; H, 3.40; N, 4.59%. ^{1}H NMR (400 MHz, $CDCl_3$): δ 7.96 (s, 2H), 7.79 (dd, J = 13.1, 7.5 Hz, 2H), 7.66–7.48 (m, 7H), 7.48–7.39 (m, 3H), 7.35–7.27 (m, 4H), 7.22 (d, J = 7.5 Hz, 1H), 7.18–7.10 (m, 2H), 7.09–7.03 (m, 2H), 6.99 (t, J = 7.7 Hz, 2H), 6.83 (td, J = 7.8, 3.2 Hz, 2H), 6.61 (d, J = 7.2 Hz, 2H). ^{31}P{^{1}H} NMR (202 MHz, $CDCl_3$): δ 8.04 (d, $^1J_{Pt-P}$ = 3581.7 Hz, $^2J_{PP}$ = 17.7 Hz), −4.06 (d, $^1J_{Pt-P}$ = 3720.7 Hz, $^2J_{PP}$ = 17.7 Hz). HRMS (ES) m/z calcd for $C_{38}H_{29}N_3P_2PtCl$ ([M − Cl])$^+$ 819.1171; found 820.1162.

Synthesis of [Au_2Cl_2\{ *o*-$Ph_2P(C_6H_4)$\{1,2,3-$N_3C(Ph)C(PPh_2)$\}\}-μ-P,P] (12)

A dichloromethane (5 mL) solution of $AuCl(SMe_2)$ (0.030 g, 0.102 mmol) was added drop wise to a solution of **2** (0.030 g,

Table 5 Crystallographic Information for compounds **8–12**

	8	**9**	**10**	**11**	**12**
Formula	$C_{87}H_{69}Cl_5N_6P_4Ru_2$	$C_{48}H_{43}Cl_2N_3P_2Ru$	$C_{39}H_{30}Cl_5N_3P_2Pd$	$C_{39}H_{30}Cl_5N_3P_2Pt$	$C_{39}H_{30}Au_2Cl_5N_3P_2$
Formula weight	1701.75	895.76	887.25	974.94	1173.78
T (K)	150	150	150	150	150
Crystal system	Triclinic	Triclinic	Monoclinic	Orthorhombic	Monoclinic
Space group	$P\bar{1}$	$P\bar{1}$	$P2_1/c$	$P2_12_12_1$	$P2_1/c$
a, Å	13.7636(3)	12.7908(7)	13.3510(4)	10.2544(3)	12.7791(5)
b, Å	14.7629(4)	15.2107(10)	11.0729(2)	12.3816(4)	14.3916(6)
c, Å	22.1839(5)	15.2959(10)	25.9296(6)	28.9853(11)	20.6657(8)
α, deg	76.1417(19)	114.525(6)	90	90	90
β, deg	85.9054(18)	103.851(5)	95.690(2)	90	95.247(4)
γ, deg	85.3961(19)	102.567(5)	90	90	90
V, Å^3	4355.90(17)	2453.6(3)	3814.38(17)	3680.1(2)	3784.7(3)
Z	2	2	4	4	4
ρ_{calc}g/cm^3	1.297	1.212	1.545	1.76	2.06
M (MoKα)/mm^{-1}	0.619	0.526	0.954	4.297	8.216
F(000)	1732	920	1784	1912	2232
Crystal size (mm^3)	0.123 × 0.102 × 0.065	0.176 × 0.153 × 0.098	0.222 × 0.091 × 0.05	0.175 × 0.157 × 0.072	0.17 × 0.07 × 0.05
Theta range (deg)	4.17 to 50	3.174 to 49.994	4.178 to 49.994	3.29 to 49.994	4.272 to 50
Reflections collected	83 601	47 691	36 825	24 542	30 848
Independent reflections	15 315	8624	6721	6484	6649
S	1.054	1.037	1.053	1.109	1.025
R_1[a]	0.0582	0.084	0.0406	0.0562	0.0269
wR_2[b]	0.1493	0.2392	0.0835	0.134	0.065

[a] $R = \Sigma||F_o| - |F_c||/\Sigma|F_o|$. [b] $wR_2 = [\Sigma w(F_o^2 - F_c^2)^2/\Sigma w(F_o^2)^2]^{1/2}$ w $= 1/[\sigma^2(F_o^2) + (xP)^2]$ where $P = (F_o^2 + 2F_c^2)/3$.

Table 6 Selected bond distances (Å) and angels (°) for compounds **4–7**

	4 (M = W)	**5** (M = Mo)	**6** (M = W)	**7** (M = W)
Bond distances				
P1–C2	1.840(4)	1.846(3)	1.844(5)	1.854(6)
P2–C7	1.824(4)	1.834(3)	1.828(5)	1.827(6)
P1–M	2.5156(11)	2.5335(9)	2.5263(13)	2.5080(15)
P2–M	—	2.5245(9)	2.5131(13)	—
M–CAvg	2.002(5)	2.017(4)	2.018(6)	2.009(6)
N1–N2	1.369(5)	1.353(4)	1.354(5)	1.360(6)
N2–N3	1.313(5)	1.303(4)	1.311(6)	1.312(6)
C39–O1	1.161(6)	1.149(5)	1.157(7)	1.141(7)
C40–O2	1.156(6)	1.147(4)	1.146(6)	1.157(7)
M–N2	2.242(3)	—	—	2.244(5)
P2–Au	—	—	—	2.2134(15)
Au–Cl	—	—	—	2.2893(15)
Bond angles				
P1–M–P2	—	87.76(3)	87.81(4)	—
P1–M–N2	75.10(9)	—	—	76.14(9)
P1–M–C40	97.74(15)	92.21(10)	92.27(16)	97.74(15)
P2–M–C39	—	92.06(10)	92.27(16)	—
N2–M–C39	96.93(18)	—	—	96.93(18)
P1–M–C39	171.68(15)	174.34(11)	173.87(15)	166.05(17)
N2–M–C40	172.32(16)	—	—	176.10(19)
P2–M–C40	—	178.17(10)	178.09(14)	—
C41–M–C42	173.32(17)	174.19(14)	174.8(2)	168.8(2)
N1–N2–N3	107.3(3)	107.4(3)	107.2(4)	108.6(4)
P2–Au–Cl	—	—	—	175.86(5)

0.051 mmol) in the same solvent (6 mL) and stirred for 4 h at room temperature. The solvent was removed under reduced pressure and the residue obtained was washed dissolved in a mixture of petroleum ether (5 mL) and chloroform (1 mL) and stored at room temperature for 24 h to give **12** as a colourless crystalline solid. Yield: 68% (0.041 g). Mp: >275 °C. Anal. calcd for $C_{38}H_{29}Au_2Cl_2N_3P_2 \cdot CHCl_3$: C, 39.91; H, 2.58; N, 3.58. Found C, 39.37; H, 2.31; N, 3.65%. ^{1}H NMR: (400 MHz, $CDCl_3$): δ 7.80–7.63 (m, 5H), 7.61–7.45 (m, 13H), 7.25 (d, J = 6.2 Hz, 3H), 7.23–7.16 (m, 2H), 7.10 (t, J = 7.4 Hz, 1H), 7.00 (ddd, J = 19.3, 11.2, 6.2 Hz, 4H), 6.58 (dd, J = 7.6, 4.7 Hz, 1H). $^{31}P\{^1H\}$ NMR (202 MHz, $CDCl_3$): δ 24.49 (s), 12.18 (s). HRMS (ES): m/z Calcd. for $C_{38}H_{29}Au_2ClN_3P_2$ ($[M - Cl]^+$): 1018.0851; found: 1018.0853.

Table 7 Selected bond distances (Å) and angels (°) for compounds **8–12**

	8 (M = Ru)	**9** (M = Ru)	**10** (M = Pd)	**11** (M = Pt)
Bond distances				
P1–M	2.2851(13)	2.3060(19)	2.2606(9)	2.249(4)
P2–M	2.2902(13)	—	2.2549(9)	2.241(4)
N2–M	—	2.136(6)	—	—
M–Cl1	2.4245(12)	2.4074(19)	2.3243(9)	2.336(4)
M–Cl2			2.3507(9)	2.352(4)
M–Cavg	2.2066	2.237	—	—
P1–C2	1.835(5)	1.825(8)	1.835(3)	1.834(17)
P2–C7	1.827(4)	1.838(8)	1.818(3)	1.853(19)
N3···H34	2.505	—	—	—
Bond angels				
P1–M–P2	91.86(5)	—	94.72(3)	94.11(16)
P1–M–N2	—	80.42(16)	—	—
P1–M–Cl1	88.72(4)	89.85(7)	93.56(3)	89.09(16)
P1–M–Cl2	—	—	168.66(3)	174.15(16)
P2–M–Cl1	93.59(4)	—	167.96(4)	171.60(16)
P2–M–Cl2	—	—	88.64(3)	90.92(16)
P1–M–P2	91.86(5)	—	94.72(3)	94.11(16)

General procedure for tandem Cu-free Sonagashira alkynylation/cyclization reaction

The reactions were performed in a closed vessel containing a mixture of alkyne (1.2 equiv.), substituted 2-iodophenol (1.0 equiv), Cs_2CO_3 (1.5 equiv) and catalyst **10** (1 mol%) in DMSO (3 mL). The reaction mixture was heated at 80 °C for 6 h. The solution was diluted with H_2O (10 mL) extracted twice with ethyl acetate (10 mL). The combined organic fractions were dried over Na_2SO_4 and the solvent was evaporated under reduced pressure. The crude product obtained was purified by silica gel column chromatography using petroleum ether/ethyl acetate.

X-ray crystallography

Single crystal X-ray data collection was performed at 100–150 K using a Rigaku Saturn724 diffractometer (Enhance Mo-Kα X-ray source, λ = 0.71073 Å) with a graphite monochromater for compounds **2** and **4–12** with the ω-scan technique. Crystal data and the details of the structure determination of **2** and **4–12** are given in Tables 4 and 5, whereas the selected bond parameters are listed in Tables 6 and 7. The data were reduced using CrysalisPro Red 171.38.43 software. The structures were solved by Olex2 (ref. 29) with the ShelXT[30] structure solution program using intrinsic phasing and refined with the ShelXL[31] refinement package using least squares minimization. All non-hydrogen atoms were refined anisotropically. Hydrogen atoms were placed in calculated positions and included as riding contributions with isotropic displacement parameters tied to those of the attached non-hydrogen atoms. In compounds **4**, **8** and **9** the disordered solvent molecules could not be identified or modelled to a known solvent hence it was SQUEEZED using PLATON.[32] Crystallographic data for the structures reported in this paper have been deposited with the Cambridge Crystallographic Data Centre as supplementary publication no. CCDC 1832214 (compound **2**) and CCDC 1832216–1832224 (compounds **4–12**).

Conflicts of interest

There are no conflicts to declare.

Acknowledgements

We are grateful to the Science & Engineering Research Board, New Delhi, India, for financial support of this work through grant No. SB/S1/IC-08/2014. LR and MKP thank UGC, New Delhi for the fellowship. We also thank the Department of Chemistry Instrumentation Facilities, IIT Bombay, for spectral and analytical data. We thank Dr Debasish Sengupta for verifying some catalytic data.

References

1 (*a*) P. Braunstein and F. Naud, *Angew. Chem., Int. Ed.*, 2001, **40**, 680–699; (*b*) R. J. Long, V. C. Gibson, A. J. P. White and D. J. Williams, *Inorg. Chem.*, 2006, **45**, 511–513; (*c*) N. Dwadnia, J. Roger, N. Pirio, H. Cattey and J.-C. Hierso, *Coord. Chem. Rev.*, 2018, **355**, 74–100.

2 E. M. Schuster, M. Botoshansky and M. Gandelman, *Organometallics*, 2009, **28**, 7001–7005.

3 M. Hirotsu, K. Santo, Y. Tanaka and I. Kinoshita, *Polyhedron*, 2018, **143**, 201–208.

4 (*a*) E. Poverenov, M. Gandelman, L. J. W. Shimon, H. Rozenberg, Y. Ben-David and D. Milstein, *Organometallics*, 2005, **24**, 1082–1090; (*b*) R. Lindner, B. van den Bosch, M. Lutz, J. N. H. Reek and J. I. van der Vlugt, *Organometallics*, 2011, **30**, 499–510; (*c*) G. Mancano, M. J. Page, M. Bhadbhade and B. A. Messerle, *Inorg. Chem.*, 2014, **53**, 10159–10170; (*d*) A. Ghisolfi, A. Waldvogel, L. Routaboul and P. Braunstein, *Inorg. Chem.*, 2014, **53**, 5515–5526.

5 (*a*) V. Balzani, A. Credi and M. Venturi, *Molecular Devices and Machines*, Wiley-VCH, New York, 2nd edn, 2008; (*b*) D. Kalny, M. Elhabiri, T. Moav, A. Vaskevich, I. Rubinstein, A. Shanzer and A.-M. Albrecht-Gary, *Chem. Commun.*, 2002, 1426–1427.

6 (*a*) J. R. Dilworth and N. Wheatley, *Coord. Chem. Rev.*, 2000, **199**, 89–158; (*b*) S. Kumar, G. Mani, S. Mondal and P. K. Chattaraj, *Inorg. Chem.*, 2012, **51**, 12527–12539.

7 (*a*) P. Espinet and K. Soulantica, *Coord. Chem. Rev.*, 1999, **193**, 499–556; (*b*) C. Zeng, N. Wang, T. Peng and S. Wang, *Inorg. Chem.*, 2017, **56**, 1616–1625.

8 (*a*) Y. Canac, N. Debono, L. Vendier and R. Chauvin, *Inorg. Chem.*, 2009, **48**, 5562–5568; (*b*) I. Abdellah, Y. Canac, C. D. Mboyi, C. Duhayon and R. Chauvin, *J. Organomet. Chem.*, 2015, **776**, 149–152; (*c*) S. A. Bhat, M. K. Pandey, J. T. Mague and M. S. Balakrishna, *Dalton Trans.*, 2017, **46**, 227–241.

9 (*a*) A. Otero, F. Carrillo-Hermosilla, P. Terreros, T. Expósito, S. Rojas, J. Fernández-Baeza, A. Antiñolo and I. López-Solera, *Eur. J. Inorg. Chem.*, 2003, **2003**, 3233–3241; (*b*) S. A. Bhat, J. T. Mague and M. S. Balakrishna, *Dalton Trans.*, 2015, **44**, 17696–17703; (*c*) S. A. Bhat, J. T. Mague and M. S. Balakrishna, *Inorg. Chim. Acta*, 2016, **443**, 243–250.

10 (*a*) T. Benincori, E. Brenna, F. Sannicolò, L. Trimarco, P. Antognazza, E. Cesarotti, F. Demartin and T. Pilati, *J. Org. Chem.*, 1996, **61**, 6244–6251; (*b*) N. G. Andersen, M. Parvez and B. A. Keay, *Org. Lett.*, 2000, **2**, 2817–2820.

11 (*a*) D. M. Zink, T. Grab, T. Baumann, M. Nieger, E. C. Barnes, W. Klopper and S. Bräse, *Organometallics*, 2011, **30**, 3275–3283; (*b*) D. M. Zink, T. Baumann, J. Friedrichs, M. Nieger and S. Bräse, *Inorg. Chem.*, 2013, **52**, 13509–13520; (*c*) D. M. Zink, D. Volz, T. Baumann, M. Mydlak, H. Flügge, J. Friedrichs, M. Nieger and S. Bräse, *Chem. Mater.*, 2013, **25**, 4471–4486.

12 (*a*) D. Liu, W. Gao, Q. Dai and X. Zhang, *Org. Lett.*, 2005, **7**, 4907–4910; (*b*) Q. Dai, W. Gao, D. Liu, L. M. Kapes and X. Zhang, *J. Org. Chem.*, 2006, **71**, 3928–3934; (*c*) R. J. Detz, S. A. Heras, R. de Gelder, P. W. N. M. van Leeuwen, H. Hiemstra, J. N. H. Reek and J. H. van Maarseveen, *Org. Lett.*, 2006, **8**, 3227–3230; (*d*) S.-i. Fukuzawa, H. Oki, M. Hosaka, J. Sugasawa and S. Kikuchi, *Org. Lett.*, 2007, **9**, 5557–5560.

13 B. Choubey, L. Radhakrishna, J. T. Mague and M. S. Balakrishna, *Inorg. Chem.*, 2016, **55**, 8514–8526.

14 L. Bonnafoux, L. Ernst, F. R. Leroux and F. Colobert, *Eur. J. Inorg. Chem.*, 2011, **2011**, 3387–3397.

15 (*a*) M. Ardon, G. Hogarth and D. T. W. Oscroft, *J. Organomet. Chem.*, 2004, **689**, 2429–2435; (*b*) D. F. Brayton and D. M. Heinekey, *Organometallics*, 2008, **27**, 3901–3906.

16 (*a*) Y. Zhao and D. G. Truhlar, *Theor. Chem. Acc.*, 2008, **120**, 215–241; (*b*) Y. Zhao and D. G. Truhlar, *Acc. Chem. Res.*, 2008, **41**, 157–167.

17 (*a*) P. Fuentealba, H. Preuss, H. Stoll and L. Von Szentpály, *Chem. Phys. Lett.*, 1982, **89**, 418–422; (*b*) D. Andrae, U. Häußermann, M. Dolg, H. Stoll and H. Preuß, *Theor. Chim. Acta*, 1990, **77**, 123–141.

18 M. J. Frisch, G. W. Trucks, H. B. Schlegel, G. E. Scuseria, M. A. Robb, J. R. Cheeseman, G. Scalmani, V. Barone, B. Mennucci, G. A. Petersson, H. Nakatsuji, M. L. Caricato, X. H. P. Hratchian, A. F. Izmaylov, J. Bloino, G. Zheng, J. L. Sonnenberg, M. Hada, M. Ehara, K. Toyota, R. Fukuda, J. Hasegawa, M. Ishida, T. Nakajima, Y. Honda, O. Kitao, H. Nakai, T. Vreven, J. A. Montgomery Jr, J. E. Peralta, F. Ogliaro, M. Bearpark, J. J. Heyd, E. Brothers, K. N. Kudin, V. N. Staroverov, R. Kobayashi, J. Normand, K. Raghavachari, A. Rendell, J. C. Burant, S. S. Iyengar, J. Tomasi, M. Cossi, N. Rega, N. J. Millam, M. Klene, J. E. Knox, J. B. Cross, V. Bakken, C. Adamo, J. Jaramillo, R. Gomperts, R. E. Stratmann, O. Yazyev, A. J. Austin, R. Cammi, C. Pomelli, J. W. Ochterski, R. L. Martin, K. Morokuma, V. G. Zakrzewski, G. A. Voth, P. Salvador, J. J. Dannenberg, S. Dapprich, A. D. Daniels, O. Farkas, J. B. Foresman, J. V. Ortiz, J. Cioslowski and D. J. Fox, *Gaussian 09, Revision A.02*, Gaussian, Inc., Wallingford, CT, 2013.

19 D. A. Zhurko and G. A. Zhurko, *ChemCraft 1.5; Plimus*, San Diego, CA, Available at http://www.chemcraftprog.com.

20 S. Leonid, *Chemissian 1.7*, 2005–2010, Available at http://www.chemissian.com.

21 I. Fleming, *Frontier Orbital and OrganicChemical Reactions*, John Wiley & Sons, New York, 1976.

22 (*a*) Q.-S. Li, C.-Q. Wan, R.-Y. Zou, F.-B. Xu, H.-B. Song, X.-J. Wan and Z.-Z. Zhang, *Inorg. Chem.*, 2006, **45**, 1888–1890; (*b*) Q.-L. Ni, X.-F. Jiang, T.-H. Huang, X.-J. Wang, L.-C. Gui and K.-G. Yang, *Organometallics*, 2012, **31**, 2343–2348.

23 R. J. Lundgren, M. A. Rankin, R. McDonald, G. Schatte and M. Stradiotto, *Angew. Chem., Int. Ed.*, 2007, **46**, 4732–4735.

24 C. K. Seubert, Y. Sun and W. R. Thiel, *Dalton Trans.*, 2009, 4971–4977.

25 H. Schmidbaur and A. Schier, *Chem. Soc. Rev.*, 2012, **41**, 370–412.

26 (*a*) J. Zhang, L. Li, Y. Wang, W. Wang, J. Xue and Y. Li, *Org. Lett.*, 2012, **14**, 4528–4530; (*b*) M. Heravi, V. Zadsirjan,

H. Hamidi and P. H. Tabar Amiri, *RSC Adv.*, 2017, **7**, 24470–24521.

27 (*a*) R. Chinchilla and C. Nájera, *Chem. Rev.*, 2007, **107**, 874–922; (*b*) R. Wang, S. Mo, Y. Lu and Z. Shen, *Adv. Synth. Catal.*, 2011, **353**, 713–718; (*c*) M. Yamaguchi, T. Akiyama, H. Sasou, H. Katsumata and K. Manabe, *J. Org. Chem.*, 2016, **81**, 5450–5463.

28 R. Zhou, W. Wang, Z.-j. Jiang, K. Wang, X.-l. Zheng, H.-y. Fu, H. Chen and R.-x. Li, *Chem. Commun.*, 2014, **50**, 6023–6026.

29 O. V. Dolomanov, L. J. Bourhis, R. J. Gildea, J. A. K. Howard and H. Puschmann, *J. Appl. Crystallogr.*, 2009, **42**, 339–341.

30 G. Sheldrick, *Acta Crystallogr., Sect. A: Found. Adv.*, 2015, **71**, 3–8.

31 G. M. Sheldrick, *Acta Crystallogr., Sect. C: Cryst. Struct. Commun.*, 2015, **71**, 3–8.

32 A. Spek, *J. Appl. Crystallogr.*, 2003, **36**, 7–13.

33 D. J. Darensbourg and R. L. Kump, *Inorg. Chem.*, 1978, **17**, 2680–2682.

34 M. I. Bruce, C. Hamiester, A. G. Swincer and R. C. Wallis, *Inorg. Synth.*, 1982, **21**, 78–82.

35 M. A. Bennett, T. N. Huang, T. W. Matheson and A. K. Smith, *Inorg. Synth.*, 1982, **21**, 74–76.

36 D. Drew and J. R. Doyle, *Inorg. Synth.*, 1990, **28**, 346–349.

37 M.-C. Brandys, M. C. Jennings and R. J. Puddephatt, *J. Chem. Soc., Dalton Trans.*, 2000, 4601–4606.

38 M. J. Bosiak, *ACS Catal.*, 2016, **6**, 2429–2434.